Design and Control of a Demand Flow System Assuring Spontaneous Breathing of a Patient Connected to an HFO Ventilator

Karel Roubík*, Jakub Ráfl, *Student Member, IEEE*, Marc van Heerde, and Dick G. Markhorst

Abstract—Lung protective ventilation is intended to minimize the risk of ventilator induced lung injury and currently aimed at preservation of spontaneous breathing during mechanical ventilation. High-frequency oscillatory ventilation (HFOV) is a lung protective ventilation strategy. Commonly used high-frequency oscillatory (HFO) ventilators, SensorMedics 3100, were not designed to tolerate spontaneous breathing. Respiratory efforts in large pediatric and adult patients impose a high workload to the patient and may cause pressure swings that impede ventilator function. A Demand Flow System (DFS) was designed to facilitate spontaneous breathing during HFOV. Using a linear quadratic Gaussian state feedback controller, the DFS alters the inflow of gas into the ventilator circuit, so that it instantaneously compensates for the changes in mean airway pressure (*MAP*) in the ventilator circuit caused by spontaneous breathing. The undesired swings in *MAP* are thus eliminated. The DFS significantly reduces the imposed work of breathing and improves ventilator function. In a bench test the performance of the DFS was evaluated using a simulator ASL 5000. With the gas inflow controlled, *MAP* was returned to its preset value within 115 ms after the beginning of inspiration. The DFS might help to spread the use of HFOV in clinical practice.

Index Terms—Demand Flow System, high-frequency oscillatory ventilation (HFOV), linear quadratic Gaussian (LQG) control, mechanical ventilation.

I. INTRODUCTION

MECHANICAL ventilation (MV) is an effective, life-saving technique for the management of patients with respiratory insufficiency or failure. Nevertheless, numerous studies have shown that MV itself can initiate as well as exacerbate lung injury and negatively affect other body organs [1]. This is known as ventilator-induced lung injury, which is the major cause of still persisting high mortality during MV. The effort to reduce the mortality leads to the development of lung protective MV strategies that can protect the already injured lung from additional harm. An important issue is not to fully take over the patient's respiration, but to allow spontaneous breathing. Spontaneous breathing during MV has clinical relevant positive effects on the diseased lung, lowers need for sedatives, and shortens duration of both MV and intensive care stay [2]. The current trend in MV is to synchronize the ventilator's activity with the breathing of a patient.

During the last decades, advances in control technology have played a major role in the evolution of MV [3]. Much effort was made to adapt ventilators to spontaneously breathing patients. The incorporation of advanced control in modern ventilators has moved the control of ventilation from the machine to the patient. New MV modes provide automatic control of ventilator output in response to patients' changing requirements. Algorithms for the assessment of successful extubation are being sought [4], and some ventilators even use optimal control algorithms to automatically wean patients from MV [3]. Research activities are also aimed at development of closed-loop MV controllers with explicit definition of target physiological parameters, such as blood oxygen saturation and concentration of CO_2 in the expired gas [5].

High-frequency oscillatory ventilation (HFOV) is a lung protective strategy very different from other modes of MV. Whereas the physiologic breathing frequency is 0.2–0.35 Hz (12–20 breaths per minute) during quiet breathing, HFOV delivers pressure oscillations of 3–15 Hz around a constant mean airway pressure (*MAP*), producing tidal volumes of approximately 1–2 mL/kg body weight [6]. These tidal volumes are often less than anatomical dead space, and associated swings in alveolar pressure are very small. This approach should theoretically limit ventilator-induced lung injury [7].

Unfortunately, ventilators for HFOV still do not offer such sophisticated control of MV as other ventilators. Spontaneous breathing of a patient is not possible during HFOV, which represents one of the most significant disadvantages of HFOV.

The SensorMedics 3100 HFO ventilator (SensorMedics, Yorba Linda, CA, USA) was developed in the early 1980s and is the most commonly used HFO ventilator in large pediatric and adult patients. These HFO ventilators use open-loop control for all ventilator settings. Spontaneous breathing was not taken into account during the design of this HFO ventilator and causes two main problems. First, vigorous respiratory effort in large pediatric and adult patients impedes HFO ventilator function. It causes pressure swings that activate alarms, interrupt oscillations, and produce significant oxygen desaturation of the blood hemoglobin. Initial HFOV trials in adults recommended muscular paralysis for this reason [8]. Second, when a patient

*K. Roubík and J. Ráfl are with the Department of Biomedical Technology, Faculty of Biomedical Engineering, Czech Technical University in Prague, Kladno, Czech Republic, CZ-272 01 (e-mail: roubik@fbmi.cvut.cz).
M. van Heerde and D. G. Markhorst are with the Department of Pediatric Intensive Care, VU University Medical Center, Amsterdam, The Netherlands.

breathes spontaneously during MV, all components of the ventilator circuit impose a resistive workload to the patient. This imposed workload caused by the HFO ventilator is rather high and makes it difficult to breathe during HFOV [9]. Nonetheless, current protocols attempt to maintain spontaneous breathing during HFOV [10].

The aim of this study is to eliminate the disadvantage of the HFOV—the impossibility of spontaneous breathing of adult patients connected to an HFO ventilator. The paper presents the design, control, and function of a device designed to facilitate spontaneous breathing during HFOV with SensorMedics 3100 HFO ventilators. The paper is organized as follows: Section II specifies the problem of spontaneous breathing during HFOV with the standard HFO ventilator and introduces the proposed solution. Section III presents the new configuration of the HFO ventilator, enhanced by a system which allows spontaneous breathing during HFOV. The hardware structure of the new system is presented. Section IV describes the control algorithm used. Section V presents the results of a bench test conducted with the designed system, and Section VI presents the result of an animal experiment. Finally, Sections VII and VIII include discussion on the system performance, limitations, and the study conclusions.

II. PROBLEM FORMULATION

A standard configuration of a SensorMedics 3100 HFO ventilator is presented in Fig. 1(a). The inspiratory gas mixture from an air-oxygen blender enters a bias flow generator in the HFO ventilator. The manually adjustable generator can deliver a fixed bias flow rate Q_{bf} between 0 and 60 L/min. This flow passes through the ventilator circuit and escapes via a balloon valve. The balloon valve represents a resistance, which, together with the bias flow, determines *MAP* in the ventilator circuit. *MAP* assures a sufficient alveolar lung surface area for gas diffusion and controls oxygenation. The generation of inspiratory and expiratory volume is provided by an oscillating membrane, operating at a frequency between 3 and 15 Hz. The oscillating membrane generates pressure swings that propagate through the ventilator circuit to the airway opening of a patient's respiratory system. These changes of pressure create a bidirectional flow of gas between the ventilator circuit and the connected airways.

The relatively low and fixed Q_{bf} is the reason that spontaneous breathing is not well tolerated during HFOV [9]. The fixed Q_{bf} results in a decrease in *MAP* during spontaneous inspiration and an increase in *MAP* during expiration. A ventilator may evaluate the pressure swings caused by the patient's breathing as a possible danger. Patient's exhalation induces an increase in *MAP* in the ventilator circuit, which may exceed the set alarm limits. As a result, the alarm is activated and, finally, the ventilator discontinues its operation. The same may occur during a patient's inhalation when a decrease in *MAP* in the ventilator circuit may be considered as a significant gas leak or circuit disconnection.

A patient's spontaneous breathing that does not affect ventilator performance may be assured by an additional device which instantaneously compensates for the swings in *MAP* induced by
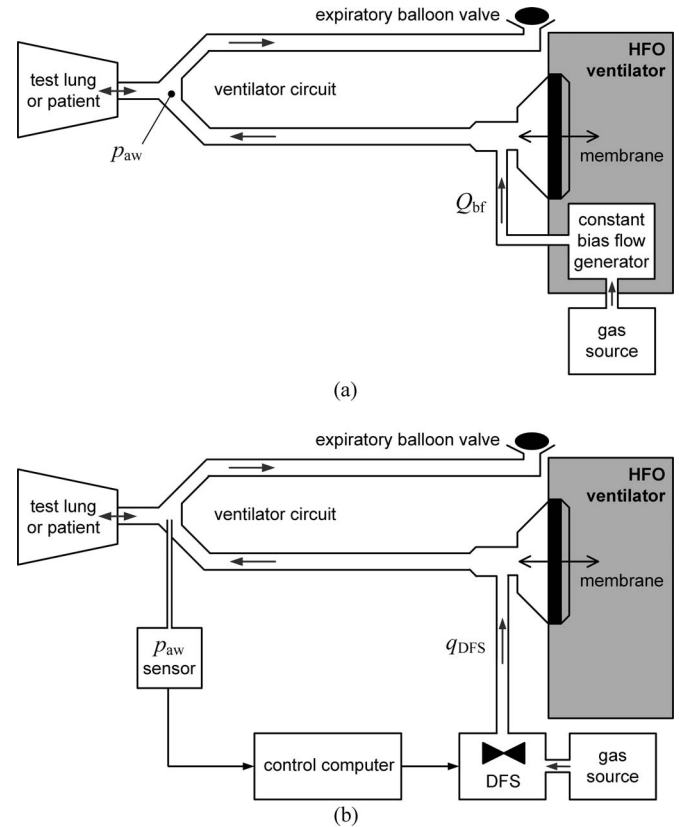
Fig. 1. High-frequency oscillatory ventilator connected to a patient in the standard configuration with constant bias flow (a) and with the Demand Flow System providing the variable gas inflow (b).

a patient's spontaneous breathing. Such a device should rapidly react to the changes in the amount of gas in the ventilator circuit. When using a fixed Q_{bf}, this amount of gas decreases as a result of a patient's inhalation and increases as a result of a patient's exhalation. A device that is able to compensate for these volume changes in the ventilator circuit would promptly eliminate the undesired pressure swings in *MAP*. We refer to such a device as the Demand Flow System (DFS).

There are two main advantages of the DFS. First, full compensation of the gas volume changes in the ventilator circuit completely eliminates *MAP* changes in the ventilator circuit caused by a patient's spontaneous breathing. As *MAP* is the only parameter monitored by the HFO ventilator, for both operational and safety reasons, functioning of the HFO ventilator will not be affected by spontaneous breathing activity.

Next, rapid compensation of gas volume changes would significantly reduce a patient's breathing workload. This has been already documented in [9] and [11]. When spontaneous breathing of a patient connected to an HFO ventilator is desired, the imposed work of breathing must be reduced. The DFS may reduce imposed workload significantly, as it easily makes available any amount of inspiratory gas upon a patient's demand. Hence, the patient does not need to overcome the high resistance components of the original HFO ventilator circuit.
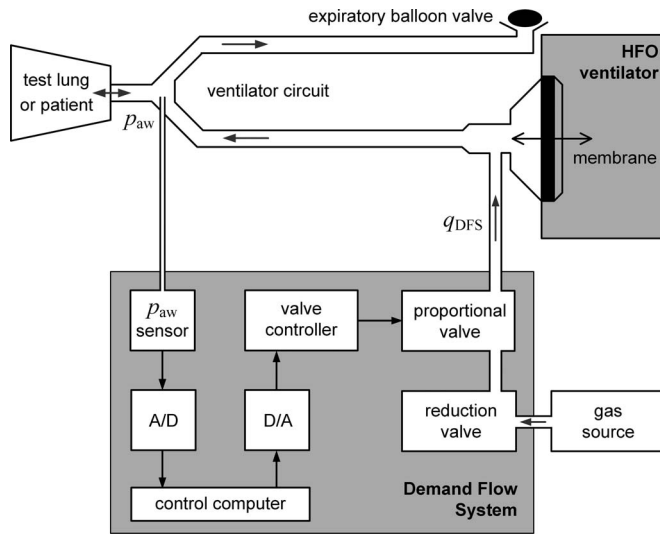
Fig. 2. Fundamental structure of the Demand Flow System.

III. DEMAND FLOW SYSTEM DESIGN

The DFS replaces the original fixed Q_{bf} through the ventilator circuit by gas flow instantaneously adjusted according to a spontaneously breathing patient.

In the new configuration, presented in Fig. 1(b), the HFO ventilator provides only the oscillations, assuring bidirectional gas flow between the ventilator circuit and a patient's lung, whereas gas flow through the ventilator circuit is completely delivered by the DFS. This system maintains the necessary bias flow and simultaneously eliminates *MAP* changes in the ventilator circuit caused by spontaneous breathing. When a patient starts to inhale, gas is removed from the ventilator circuit, which leads to a drop in *MAP*, detected by a pressure sensor. In response, the DFS increases the gas flow rate q_{DFS} into the ventilator circuit so that the flow through the expiratory balloon valve is returned to its original value, and therefore *MAP* in the circuit is maintained constant. Similarly, reduction of gas inflow into the circuit maintains *MAP* unaltered during spontaneous exhalation. As a result, *MAP* does not change regardless of a patient's spontaneous breathing effort.

The fundamental structure of the DFS is depicted in Fig. 2. The pressure sensor (14PC03D, Honeywell, USA) converts the proximal airway pressure p_{aw}, measured at the proximal end of the endotracheal tube, to an analog voltage signal. The voltage signal is sampled and digitized by an A/D converter in a data acquisition board (DAQCard-6024E, National Instruments Corporation, Austin, TX, USA) and sent to a control computer, where it is converted into a discrete proximal airway pressure signal $p_{aw}(k)$ at a discrete time k. A control algorithm (described in the next section) realized in the MATLAB/Simulink environment (The MathWorks, Nattick, MA, USA) calculates the desired discrete value of the gas flow rate $q_{DFS}(k)$. Voltage necessary for the proportional valve control is derived from the $q_{DFS}(k)$ value using the conversion curve of the proportional valve. The discrete value of the control voltage is converted into an analog voltage control signal by the same data acquisition

board. After its D/A conversion, the analog voltage signal enters a micro driver that actuates the proportional valve so that the desired gas flow rate q_{DFS} can be delivered into the ventilator circuit. The valve, with a transition time 30 ms (10%–90%), was obtained from a mechanical ventilator AVEA (CareFusion, Yorba Linda, CA, USA).

The DFS operates in two modes referred to as MANUAL and DEMAND. In the MANUAL mode, *MAP* value is acquired as a 3 s moving average of p_{aw}. This measured *MAP* value serves as the target *MAP* value for the regulator during the DEMAND mode of operation. In the MANUAL mode the gas flow rate is constant; it is set by a potentiometer. This value of the flow rate is stored as the static Q_{bf} when the DFS is switched to the DEMAND mode. In the DEMAND mode, the variable component of the gas flow is automatically computed, based on the difference between the current proximal airway pressure p_{aw} and the target *MAP* value. The proportional valve is adjusted so that the total flow rate into the system is the sum of the static Q_{bf} rate and the calculated variable flow rate component.

IV. DEMAND FLOW SYSTEM CONTROL

DFS controls pressure in the ventilator circuit by means of the variable gas inflow into the circuit. The control program calculates the discrete value of the gas flow rate $q_{DFS}(k)$, based on the knowledge of the discrete proximal airway pressure signal $p_{aw}(k)$. A discrete-time linear quadratic Gaussian (LQG) state feedback controller was employed; i.e., a combination of a linear quadratic (LQ) state-feedback regulator and a state observer estimating the unknown state of a system with Gaussian stochastic disturbances. The controller is designed as a regulator that rejects the disturbances to the $p_{aw}(k)$ signal caused by spontaneous breathing.

The selected state-space approach to control requires an internal model of a regulated system, of which the main part is a model of a patient-ventilator system (the process model). The state-variable representation of the process was derived for the time-varying components of the gas flow rate q_{DFS} and the proximal airway pressure p_{aw}. A discrete-time version of this arrangement was utilized by the LQG controller.

A. Process Model

A simple linear lumped-parameter model of the regulated patient-ventilator system is presented in Fig. 3. The model was created using an electro-acoustic analogy. In this model, an RC network, together with pressure and gas-flow sources, is used to approximate the behavior of a patient's respiratory system, the HFO ventilator, and the ventilator circuit [12]. A patient's respiratory system is modeled by resistor R_1, representing the sum of airway and endotracheal tube resistance, and by capacitor C_1, representing the respiratory system compliance. The patient's spontaneous breathing is modeled by the source of pressure p_{spont}. Mechanical properties of an HFO ventilator are described by resistor R_2, representing the airflow resistance of the ventilator chamber, and by capacitor C_2, representing its compliance. The oscillations generated by the ventilator are introduced into the model using the pressure source p_{HFO}.
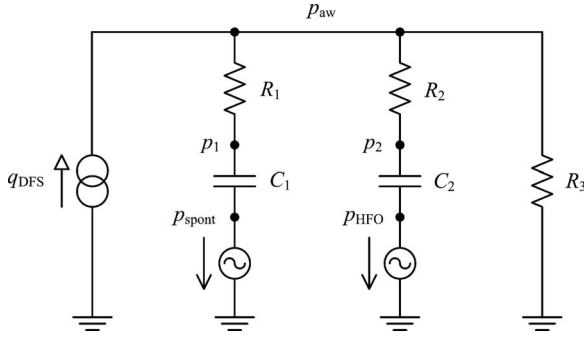
Fig. 3.   Model of the regulated patient-ventilator system.

Concerning the ventilator circuit, the most significant mechanical property is exhibited by the expiratory balloon valve, which is, together with the expiratory circuit resistance, modeled by resistor R_3. Gas inflow into the ventilator circuit from the DFS is modeled by the controlled gas flow source q_{DFS}. The pressure nodes between their respective resistors and capacitors are denoted as p_1 and p_2. Finally, the last remaining node in the model refers to the proximal airway pressure p_{aw}. For the pressures p_1, p_2, and p_{aw}, the node equations can be derived in form:

$$\frac{p_1 - p_{\mathrm{aw}}}{R_1} + C_1 \frac{d(p_1 - p_{\mathrm{spont}})}{dt} = 0 \tag{1}$$

$$\frac{p_2 - p_{\mathrm{aw}}}{R_2} + C_2 \frac{d(p_2 - p_{\mathrm{HFO}})}{dt} = 0 \tag{2}$$

$$- q_{\mathrm{DFS}} + \frac{p_{\mathrm{aw}} - p_1}{R_1} + \frac{p_{\mathrm{aw}} - p_2}{R_2} + \frac{p_{\mathrm{aw}}}{R_3} = 0. \tag{3}$$

As has already been mentioned, the constant gas flow q_{DFS} with the output resistor R_3 assures the constant value of *MAP* when a stable state is not disturbed by a patient's respiratory effort. That is, $p_{\mathrm{aw}} = MAP = R_3 Q_{\mathrm{bf}}$ when $q_{\mathrm{DFS}} = Q_{\mathrm{bf}}$, where Q_{bf} is the static bias flow. However, in a general case, the instantaneous value of the proximal airway pressure p_{aw} may differ from *MAP* by Δp_{aw}:

$$p_{\mathrm{aw}} = MAP + \Delta p_{\mathrm{aw}} = R_3 Q_{\mathrm{bf}} + \Delta p_{\mathrm{aw}}. \tag{4}$$

Accordingly, p_1 and p_2 may be expressed as

$$\begin{aligned} p_1 &= MAP + \Delta p_1 = R_3 Q_{\mathrm{bf}} + \Delta p_1 \\ p_2 &= MAP + \Delta p_2 = R_3 Q_{\mathrm{bf}} + \Delta p_2. \end{aligned} \tag{5}$$

The instantaneous value of the gas flow rate q_{DFS} controlled by the DFS may also differ from the static bias flow:

$$q_{\mathrm{DFS}} = Q_{\mathrm{bf}} + \Delta q_{\mathrm{DFS}}. \tag{6}$$

If (4)–(6) are substituted into (1)–(3), the system equations for a state vector $\Delta \mathbf{p}_{12} = [\Delta p_1 \quad \Delta p_2]^{\mathrm{T}}$ can be derived as:

$$\Delta \dot{\mathbf{p}}_{12} = \mathbf{F} \Delta \mathbf{p}_{12} + \mathbf{G} \Delta q_{\mathrm{DFS}} + \mathbf{w} \tag{7}$$

$$\Delta p_{\mathrm{aw}} = \mathbf{H} \Delta \mathbf{p}_{12} + R \Delta q_{\mathrm{DFS}} \tag{8}$$

where

$$\mathbf{F} = \begin{bmatrix} \frac{G_1^2 - G_1 G}{G C_1} & \frac{G_1 G_2}{G C_1} \\ \frac{G_1 G_2}{G C_2} & \frac{G_2^2 - G_2 G}{G C_2} \end{bmatrix}, \quad \mathbf{G} = \begin{bmatrix} \frac{G_1}{G C_1} & \frac{G_2}{G C_2} \end{bmatrix}^{\mathrm{T}}$$

$$\mathbf{w} = [\dot{p}_{\mathrm{spont}} \quad \dot{p}_{\mathrm{HFO}}]^{\mathrm{T}}, \mathbf{H} = \begin{bmatrix} \frac{G_1}{G} & \frac{G_2}{G} \end{bmatrix}, R = \frac{1}{G}$$

$$G_1 = \frac{1}{R_1}, G_2 = \frac{1}{R_2}, G_3 = \frac{1}{R_3}, G = G_1 + G_2 + G_3.$$

The actual values of the parameters used in the model are presented in APPENDIX.

Equations (7), (8) describe a linear, time-invariant, continuous-time system with the input variable flow Δq_{DFS} and the output pressure Δp_{aw}, which is the difference between the *MAP* and the actual p_{aw}. The bias flow Q_{bf} does not influence the state vector $\Delta \mathbf{p}_{12}$. The system state is, however, affected by the first time derivatives of a patient's spontaneous breathing and high-frequency oscillations, i.e., by the vector $\mathbf{w}$. The controller handles $\mathbf{w}$ as process noise causing stochastic perturbations in the system state.

The continuous-time state-space model given by (7) and (8) has been discretized with a sampling rate of $T_{\mathrm{s}} = 200\,\mathrm{Hz}$. The equivalent discrete-time equations are:

$$\Delta \mathbf{p}_{12}(k+1) = \mathbf{\Phi} \Delta \mathbf{p}_{12}(k) + \mathbf{\Gamma} \Delta q_{\mathrm{DFS}}(k) + \mathbf{w}(k) \tag{9}$$

$$\Delta p_{\mathrm{aw}}(k) = \mathbf{H} \Delta \mathbf{p}_{12}(k) + R \Delta q_{\mathrm{DFS}}(k) \tag{10}$$

where $\Delta \mathbf{p}_{12}(k) = [\Delta p_1(k) \quad \Delta p_2(k)]^{\mathrm{T}}$, $\mathbf{\Phi} = \exp\{\mathbf{F} T_{\mathrm{s}}\}$, and $\mathbf{\Gamma} = (\int_0^{T_{\mathrm{s}}} \exp\{\mathbf{F} \tau\} d\tau) \mathbf{G}$. The matrices $\mathbf{\Phi}$ and $\mathbf{\Gamma}$ have been derived from matrices $\mathbf{F}$ and $\mathbf{G}$ in a standard way by solving (7) for discrete time points $k T_{\mathrm{s}}$ and $(k+1) T_{\mathrm{s}}$, and further assuming that Δq_{DFS} is constant between the time points [13].

B. Controller Design

The p_{aw} signal consists of three principal components; two of them are variable in time and one is constant. The variable pressure components are the high-frequency oscillations produced by the HFO ventilator and the pressure swings caused by spontaneous breathing. These patient-induced pressure swings contain predominantly lower frequency components than the high-frequency oscillations. The two variable pressure components are superimposed on a steady value of *MAP*. The control algorithm separates the constant *MAP* value and the high-frequency oscillations from $p_{\mathrm{aw}}(k)$. The remaining pressure signal comprises the spontaneous breathing component only and has to be suppressed by the controller.

The implemented signal-processing procedure can be followed in Fig. 4. First, $\Delta p_{\mathrm{aw}}(k)$ is computed by subtracting the known target value of *MAP* from the discrete-time output of the process $p_{\mathrm{aw}}(k)$. Then, the high-frequency pressure oscillations are removed using a low-pass, second order discrete Butterworth filter with a cutoff frequency of 1.5 Hz. The discrete-time output signal $e(k)$ of the filter represents the undesired perturbation in the proximal airway pressure signal due to the spontaneous breathing. The objective of the LQ regulator with the feedback gain vector of $-\mathbf{K}$ is to minimize the filter output signal $e(k)$.

The LQ regulator calculates the variable discrete flow-rate component $\Delta q_{\mathrm{DFS}}(k)$ that minimizes the quadratic loss
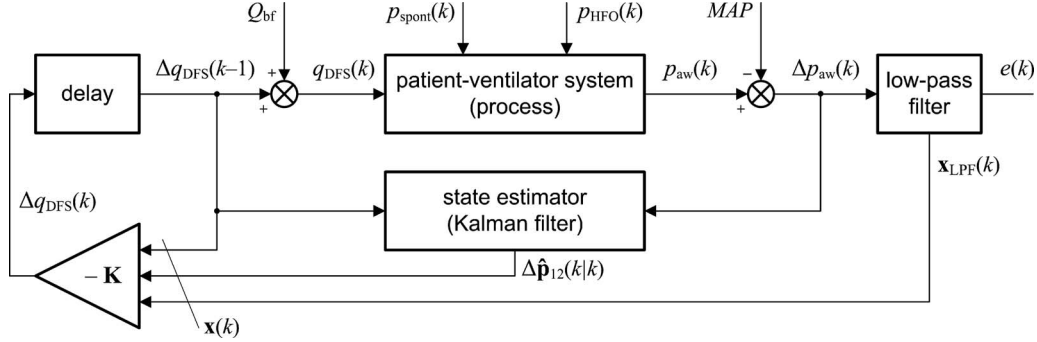
Fig. 4. Block diagram of the Demand Flow System control algorithm.

function J_{LQ} :

$$J_{\mathrm{LQ}} = \sum_{k=0}^{\infty} \left(e^{\mathrm{T}}(k) Q_{\mathrm{e}} e(k) + \Delta q_{\mathrm{DFS}}(k)^{\mathrm{T}} Q_{\mathrm{q}} \Delta q_{\mathrm{DFS}}(k) \right)$$

(11)

where Q_{e} and Q_{q} are positive weighting parameters. A one-step delay block was placed after the LQ gain block to prevent an algebraic loop. The desired discrete value of the total gas flow rate is calculated as $q_{\mathrm{DFS}}(k) = Q_{\mathrm{bf}} + \Delta q_{\mathrm{DFS}}(k-1)$.

A system controlled by the LQG controller is a serial connection of the delay block, the patient-ventilator system, and the low-pass filter. In the process model, *MAP*, determined by Q_{bf} and R_3, is completely separated from proximal airway pressure swings Δp_{aw}. Therefore, the steady components *MAP* and Q_{bf} are not relevant for the process of regulation, and for the LQG controller the patient-ventilator system is represented by (9) and (10).

The LQ regulator requires the full state information of the controlled system. As the process variables p_1 and p_2 cannot be measured and as the state $\Delta \mathbf{p}_{12}(k)$ is subject to the stochastic perturbation $\mathbf{w}(k)$ according to (9), a linear state estimator—the Kalman filter—is used to estimate $\Delta \mathbf{p}_{12}(k)$ from the process input and the process output as $\Delta \hat{\mathbf{p}}_{12}(k|k)$. The separation theorem guarantees that the LQ regulator can be designed independently of the Kalman filter as if the full-state information was available [13]. For the LQ regulator, the process is represented by the deterministic part of (9), i.e., without the vector $\mathbf{w}(k)$.

The system controlled by the LQ regulator can be described by the following equations:

$$\mathbf{x}(k+1) = \mathbf{A}\mathbf{x}(k) + \mathbf{B}\Delta q_{\mathrm{DFS}}(k)$$

(12)

$$e(k) = \mathbf{C}\mathbf{x}(k)$$

(13)

where $\mathbf{A} = \begin{bmatrix} 0 & 0 & 0 \\ \boldsymbol{\Gamma} & \boldsymbol{\Phi} & \mathbf{0} \\ \mathbf{B}_{\mathrm{LPF}}R & \mathbf{B}_{\mathrm{LPF}}\mathbf{H} & \mathbf{A}_{\mathrm{LPF}} \end{bmatrix}$, $\mathbf{B} = [1 \quad 0 \quad 0$ $0 \quad 0]^{\mathrm{T}}$, and $\mathbf{C} = [\mathbf{D}_{\mathrm{LPF}}R \quad \mathbf{D}_{\mathrm{LPF}}\mathbf{H} \quad \mathbf{C}_{\mathrm{LPF}}]^{\mathrm{T}}$. $\mathbf{0}$ is null matrix. The matrices $\mathbf{A}_{\mathrm{LPF}}$, $\mathbf{B}_{\mathrm{LPF}}$, $\mathbf{C}_{\mathrm{LPF}}$, and $\mathbf{D}_{\mathrm{LPF}}$ originate in the state-space representation of the low-pass Butterworth filter. The state vector $\mathbf{x}(k)$ consists of the state of the delay block $x_{\mathrm{d}}(k) = \Delta q_{\mathrm{DFS}}(k-1)$, the process state estimate $\Delta \hat{\mathbf{p}}_{12}(k|k)$, and the low-pass filter state $\mathbf{x}_{\mathrm{LPF}}(k)$: $\mathbf{x}(k) = [\Delta q_{\mathrm{DFS}}(k-1) \quad \Delta \hat{\mathbf{p}}_{12}(k|k) \quad \mathbf{x}_{\mathrm{LPF}}(k)]^{\mathrm{T}}$.

The loss function (11) can thus be rewritten as

$$J_{\mathrm{LQ}} = \sum_{k=0}^{\infty} \left(\mathbf{x}^{\mathrm{T}}(k)\mathbf{Q}(k) + \Delta q_{\mathrm{DFS}}(k)^{\mathrm{T}} Q_{\mathrm{q}} \Delta q_{\mathrm{DFS}}(k) \right) \quad (14)$$

where $\mathbf{Q} = \mathbf{C}^{\mathrm{T}} Q_{\mathrm{e}} \mathbf{C}$ is a positive symmetric semidefinite weighting matrix.

A solution to the LQ problem is a linear control law in the form of

$$\Delta q_{\mathrm{DFS}}(k) = -\mathbf{K}\mathbf{x}(k). \quad (15)$$

The regulator constant gain $\mathbf{K}$ is calculated from

$$\mathbf{K} = [Q_{\mathrm{q}} + \mathbf{B}^{\mathrm{T}}\mathbf{S}\mathbf{B}]^{-1}\mathbf{B}^{\mathrm{T}}\mathbf{S}\mathbf{A} \quad (16)$$

where $\mathbf{S}$ is a solution of the algebraic Riccati equation [13], [14]:

$$\mathbf{S} = \mathbf{A}^{\mathrm{T}}\mathbf{S}\mathbf{A} - \mathbf{A}^{\mathrm{T}}\mathbf{S}\mathbf{B}[Q_{\mathrm{q}} + \mathbf{B}^{\mathrm{T}}\mathbf{S}\mathbf{B}]^{-1}\mathbf{B}^{\mathrm{T}}\mathbf{S}\mathbf{A} + \mathbf{Q}. \quad (17)$$

Values of the weights used for the LQ regulator are presented in APPENDIX.

The Kalman filter generates the *a posteriori* estimate $\Delta \hat{\mathbf{p}}_{12}(k|k)$, which in each time step minimizes the criterion:

$$J_{\mathrm{KF}} = \mathrm{E}[(\Delta \mathbf{p}_{12}(k) - \Delta \hat{\mathbf{p}}_{12}(k|k))^{\mathrm{T}}(\Delta \mathbf{p}_{12}(k) - \Delta \hat{\mathbf{p}}_{12}(k|k))]$$

$$= \mathrm{Tr}\left\{ \mathrm{E}[(\Delta \mathbf{p}_{12}(k) - \Delta \hat{\mathbf{p}}_{12}(k|k))(\Delta \mathbf{p}_{12}(k) - \Delta \hat{\mathbf{p}}_{12}(k|k))^{\mathrm{T}}] \right\}$$

$$= \mathrm{Tr}\left\{ \mathbf{P}(k|k) \right\} \quad (18)$$

where $\mathrm{Tr}\{\}$ denotes the matrix trace operator and $\mathbf{P}(k|k)$ is the covariance of the estimation error of $\Delta \hat{\mathbf{p}}_{12}(k|k)$. The Kalman filter assumes a stochastic linear discrete-time single-input single-output system given by (9) and by

$$\Delta p_{\mathrm{aw}}(k) = \mathbf{H}\Delta \mathbf{p}_{12}(k) + R\Delta q_{\mathrm{DFS}}(k) + v(k) \quad (19)$$

with $\mathbf{w}(k)$ in (9) and $v(k)$ in (19) being white, zero-mean, and mutually independent discrete-time Gaussian stochastic processes. The process noise $\mathbf{w}(k)$ and the measurement noise $v(k)$ have positive semidefinite covariance matrices $\mathbf{W}$ and $\mathbf{V}$, respectively:

$$\mathrm{E}[w(k)w(j)^{\mathrm{T}}] = \mathbf{W}\delta(k-j)$$

$$\mathrm{E}[v(k)v(j)^{\mathrm{T}}] = \mathbf{V}\delta(k-j)$$

$$\mathrm{E}[w(k)v(j)^{\mathrm{T}}] = \mathbf{0} \quad (20)$$

where $\delta(k-j) = 1$ for $k = j$, otherwise $\delta(k-j) = 0$.

The Kalman filter estimates the state vector $\Delta\hat{\mathbf{p}}_{12}(k|k)$ as follows:

$$\Delta\hat{\mathbf{p}}_{12}(k|k) = \Delta\hat{\mathbf{p}}_{12}(k|k-1)$$
$$+ \mathbf{L}[\Delta p_{aw}(k) - \mathbf{H}\Delta\hat{\mathbf{p}}_{12}(k|k-1) - R\Delta q_{DFS}(k)] \quad (21)$$

where

$$\Delta\hat{\mathbf{p}}_{12}(k|k-1) = \boldsymbol{\Phi}\Delta\hat{\mathbf{p}}_{12}(k-1|k-1) + \boldsymbol{\Gamma}\Delta q_{DFS}(k-1) \quad (22)$$

is the *a priori* estimate of the state vector before the measurement $\Delta p_{aw}(k)$ is taken into account, and $\mathbf{L}$ is the innovation gain, steady-state value of which can be evaluated offline before the filter operates [13], [15]. Values of $\mathbf{W}$ and $\mathbf{V}$ used in the model are listed in APPENDIX.

Due to the nonzero direct transmission term $R \neq 0$ in the process model (19), $\Delta p_{aw}(k)$ depends directly on the input $\Delta q_{DFS}(k)$ as does the state estimate $\Delta\hat{\mathbf{p}}_{12}(k|k)$ according to (21). The state estimate should be, however, used to set $\Delta q_{DFS}(k)$ due to the LQ controller feedback law expressed by (15). To avoid the algebraic loop, the one-step delay block was integrated into the regulator state feedback. As can be seen in Fig. 4, the output of the LQ gain block is the flow rate $\Delta q_{DFS}(k)$, yet the Kalman filter estimates the system state $\Delta\hat{\mathbf{p}}_{12}(k|k)$ from the process input $\Delta q_{DFS}(k-1)$ and the process output $\Delta p_{aw}(k)$.

V. BENCH TEST

A breathing simulator ASL 5000 ACTIVE SERVO LUNG (IngMar Medical, Pittsburgh, PA, USA) was used to test the performance of the DFS during HFOV and for verifying the function of the controller. The objective of the experiment was to evaluate the ability of the DFS to maintain constant *MAP* during simulated spontaneous inspiration and expiration.

The ASL 5000 is a lung simulator that has frequently been used for ventilator testing as a model of an active respiratory system [16]–[19]. The principal component of the breathing simulator is a moving piston in a cylinder, precisely controlled by a computer. The change of volume and pressure in the cylinder due to the piston movement generates the desired breathing pattern and mimics mechanical properties of the respiratory system according to the adjusted mechanical parameters.

During the experiment, the breathing simulator was connected to a SensorMedics 3100B ventilator [Fig. 1(b)]. The interconnection consisted of a CURITY tracheal tube number 8 (Kendall-Gammatron, Sampran, Thailand), an orifice flow sensor [20], and a parabolic pneumatic resistor Rp5 (Michigan Instruments, Grand Rapids, MI, USA) simulating resistance of the real adult respiratory system. The breathing simulator was operated in the SmartPump mode as a flow pattern generator.

Step changes in flow rate q_{aw} between the ventilator circuit and the lung simulator were applied to mimic the worst possible breathing patterns of spontaneous breathing. The ideal preset flow pattern is shown in upper charts of Figs. 5 and 6. The inspiration was simulated by a sudden increase in gas flow into the simulator from the ventilator circuit. A constant inspiratory flow rate of 30 L/min was held for 3 s. After another 3 s period
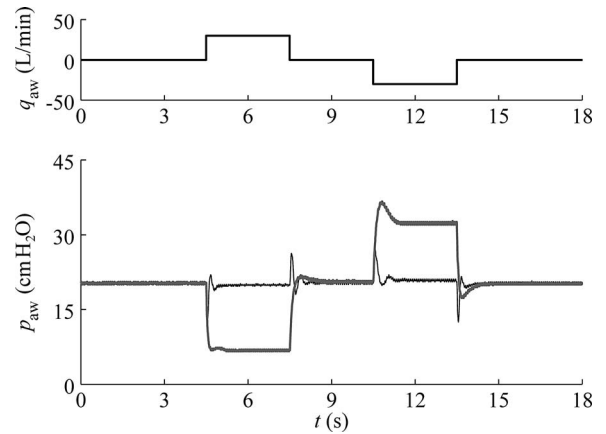
Fig. 5.   Ideal flow pattern between the ventilator circuit and the simulator ASL 5000 (upper chart) and the proximal airway pressure measured for suppressed high-frequency oscillations (lower chart). The proximal pressure was measured with the DFS switched ON (black line) and OFF (gray line).
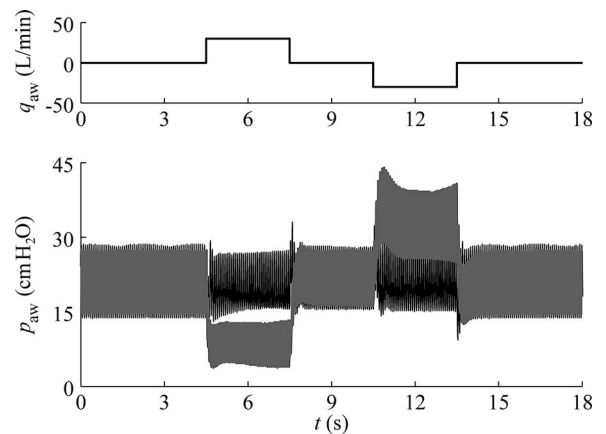
Fig. 6.   Ideal flow pattern between the ventilator circuit and the simulator ASL 5000 (upper chart) and the proximal airway pressure measured for high-frequency oscillations at frequency 15 Hz and amplitude 15 cm H_2O (lower chart). The proximal pressure was measured with the DFS switched ON (black line) and OFF (gray line).

of zero flow, 3 s reverse gas flow from the simulator into the ventilator circuit was introduced in order to simulate a patient's exhalation.

Fig. 5 presents results of a test with the high-frequency oscillations suppressed in amplitude. Fig. 6, on the other hand, presents the test results for the amplitude of high-frequency oscillations set to 15 cm H_2O and oscillatory frequency set to 15 Hz. In both tests Q_{bf} was 40 L/min and the *MAP* value was 20 cm H_2O. Lower charts in Figs. 5 and 6 compare the proximal airway pressure waveforms of a system with the DFS in the MANUAL mode (gray line)—where the DFS controller was inactive—and of a system in the DEMAND mode (black line)—where the DFS was active.

With the DFS controller inactive, *MAP* decreased approximately by 13 cm H_2O during simulated inspiration and increased approximately by 12 cm H_2O during expiration. On the contrary, with the DFS in operation *MAP* changed briefly at the beginning of inspiration and expiration, but was always returned to its preset value, followed by slight oscillations.

TABLE I
COMPARISON OF VENTILATORY PARAMETERS DURING HFOV IN PIGS
WITHOUT AND WITH THE DFS

Ventilatory parameters	Without DFS	With DFS
$iWOB$ (J/L)	0.417 ± 0.049	0.071 ± 0.009
V_T (L)	0.196 ± 0.013	0.296 ± 0.031
Minute ventilation (L/min)	4.25	5.77

The DFS trigger performance was assessed from the reaction to simulated inspiration with high-frequency oscillations suppressed. The same evaluation criteria were applied as in [21]: triggering delay and inspiratory delay. The triggering delay, defined as the time between the start of simulated breathing effort and the maximum drop in p_{aw}, was 50 ms. The inspiratory delay, defined as the time between the start of simulated breathing effort and the time when p_{aw} reached the *MAP* level again, was 115 ms.

VI. ANIMAL EXPERIMENT

In order to test the effectiveness of the DFS, an experiment on 8 Dalland pigs (53 ± 6.5 kg) were conducted. This study was approved by the Animal Welfare Committee of the VU (Vrije Universiteit) University Medical Center, Amsterdam.

After induction of anesthesia (0.5 mg atropine, 0.5 mg/kg midazolam and 10 mg/kg ketamine i.m.), an ear vein was cannulated and propofol 3 mg/kg was injected before endotracheal intubation with a cuffed tube (i.d. 8 mm). Anesthesia was maintained with continuous infusion of propofol 4 mg/(kg·h) and remifentanil 0.4 μg/(kg·min) during instrumentation. When appropriate, spontaneous breathing was suppressed with pancuronium bromide 0.3 mg/(kg·h). Arterial and venous access was assured for arterial blood gas sampling and to infuse fluids and anesthetics. Animals were placed in supine position on a heated table; body temperature was kept in the normal range (38–39 °C). In order to simulate a lung disease, surfactant deficiency was induced by a single whole lung lavage with 30–40 mL/kg 37 °C normal saline at 5 kPa, followed by a 1 h stabilization period of MV with a Servo 900 C ventilator (Maquet Critical Care AB, Solna, Sweden) in volume-controlled mode with the following settings: frequency 20 breaths per minute, inspiratory pause time 0.6 s, positive end-expiratory pressure 0.5 kPa, inspiration to expiration ratio 1:2, tidal volume 10 mL/kg was adjusted to maintain normocapnia ($PaCO_2$ 38–45 mm Hg) and pure oxygen was used for ventilation. Lavage was repeated after 1 h, after which the ventilator settings remained unchanged for 30 min.

In order to evaluate the DFS effects, the animal was switched to a SensorMedics 3100B HFO ventilator equipped with the DFS. To allow spontaneous breathing, propofol dosage was lowered to 2 mg/(kg·h), remifentanil to 0.05–0.1 μg/(kg·min). Airway pressure p_{aw} was measured at the distal end of the endotracheal tube and the corresponding airflow was recorded. From these measured variables, the spontaneous tidal volume V_T and imposed work of breathing $iWOB$ were calculated and
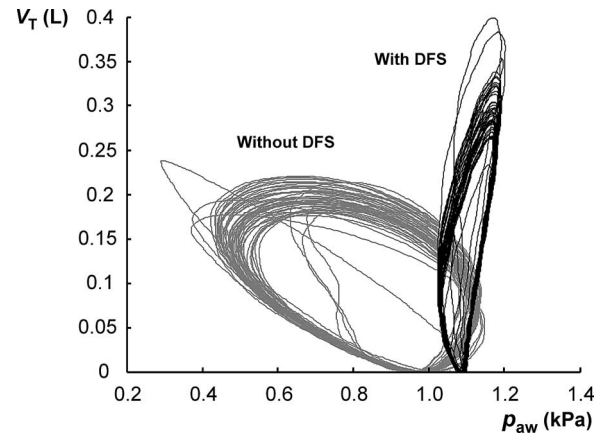
Fig. 7. Pressure-volume loops recorded in a spontaneously breathing pig connected to HFO ventilator using a standard configuration and with the DFS.

compared during HFOV with the standard configuration and during HFOV with the DFS.

Changes of spontaneous breathing parameters during HFOV before and after introduction of the DFS are summarized in Table I.

The main effects of the DFS upon the spontaneous breathing parameters are demonstrated in a form of pressure-volume loops in Fig. 7. The figure shows a remarkable reduction of p_{aw} swings and a significant increase in spontaneous V_T. As the area of each pressure-volume loop represents $iWOB$, the reduction of this area when the DFS was in operation implies a significant reduction in $iWOB$.

Use of the DFS reduced $iWOB$ by 83% ($p < 0.001$) and increased spontaneous V_T by 51% ($p < 0.001$). The DFS increased minute ventilation of the spontaneously breathing pigs by 36% ($p < 0.001$).

VII. DISCUSSION

A unique system supporting spontaneous breathing of a patient connected to an HFO ventilator has been designed. According to the results of the completed bench test, the system is able to maintain a constant value of *MAP* in a ventilator circuit regardless of spontaneous breathing activity of a ventilated patient. This has two important benefits. From the patient's perspective, spontaneous breathing requires less effort and should be better tolerated during HFOV. This could theoretically limit the commonly needed use of heavy sedation and application of muscular paralysis during HFOV in clinical practice. Next to this, a stable *MAP* assures undisturbed HFO ventilator function.

The response of the DFS to simulated inspiration and expiration is presented in Fig. 5 for the model case when the ventilator does not produce any high-frequency oscillations and, in Fig. 6, for a real situation with high-frequency oscillations. The figures show the ability of the DFS to maintain *MAP* constant. The DFS trigger performance is similar to the performance of modern ventilators currently used in clinical practice. The triggering delay of the DFS was 50 ms and is as fast as modern mechanical ventilators [21]. The inspiratory delay was 115 ms, compared to 94 ms reported for modern ventilators.

Transient pressure peaks in the p_{aw} signal develop as a reaction to sudden change in gas flow through the respiratory system. A rectangular pattern of the gas flow was selected as the worst possible (and theoretical only) waveform. In a real respiratory system, the change in the gas flow is more gradual, thus the transient peaks will be significantly less expressed. Moreover, the fast pressure swings during the transient response contain high-frequency spectral components which do not propagate deep into the respiratory system [23].

The recorded pressure signals presented in Fig. 6 document a change in amplitude of high-frequency oscillations generated by an HFO ventilator during spontaneous breathing simulation. The change in amplitude of the oscillations is caused by two combined phenomena. First, the ventilator as a source of the oscillations works into a changing load impedance. The load impedance changes especially due to the internal volume variation inside the lung simulator, directly determining the load compliance. Second, due to the nonlinearity of the HFO ventilator, the oscillating membrane exhibits different movements with changes in *MAP*, thus producing different pressure amplitudes.

The fundamental requirement of the designed control system is to separate the high-frequency oscillations from spontaneous breathing in the proximal airway pressure signal. According to Fig. 6, the changes in *MAP* are suppressed while the high-frequency oscillations are preserved. The high-frequency oscillations are separated from the spontaneous breathing signal by a low-pass Butterworth filter with a cutoff frequency of 1.5 Hz. Energy of the high-frequency oscillations is concentrated at frequencies higher than 1.5 Hz. Nevertheless, the spontaneous breathing band is not limited to frequencies under 1.5 Hz. When the signal related to a patient's spontaneous breathing contains higher frequency components, which occur during sudden changes in p_{aw}, these transient high-frequency components cannot be fully suppressed by the DFS.

The performance of the LQG controller depends on the accuracy of the model used for the description of the controlled system. Imperfections in the process model may be the reason why small swings in p_{aw} are observed when the high-frequency oscillations are switched OFF and the flow due to spontaneous breathing is zero (Fig. 5). The present model handles both the spontaneous breathing swings and the high-frequency oscillations as white, zero-mean Gaussian stochastic processes. This assumption is inaccurate, especially for high-frequency oscillations. A more precise description of the high-frequency oscillation properties may improve the process state estimation. Furthermore, the model does not consider inertial properties of gas which are not insignificant during HFOV, when moving gas matter changes its velocity rapidly. An improved model should, therefore, contain inertances. Finally, the model assumes a linear relationship between *MAP* and the bias flow in the ventilator circuit. Nevertheless, the resistance of the expiratory balloon valve of the HFO ventilator changes with variations in *MAP*, which cannot be taken into consideration in the linear model used in the DFS.

In addition to keeping *MAP* constant, there was a requirement that DFS should significantly reduce *iWOB* and, therefore, make the spontaneous breathing easier for a patient.

The positive effects of the DFS on ventilatory and physiological parameters have been tested during the animal experiment. The results of the study demonstrate that the DFS facilitates spontaneous breathing and significantly reduces *iWOB* during HFOV by more than 80%. The amount of support during spontaneous breathing can be influenced, in this setup, by changing the pressure-sampling site to regulate the DFS. Even additional pressure support can be generated to overcome *iWOB* caused by the endotracheal tube and physiologic work of breathing. The study confirms the former bench test results.

As spontaneous breathing during HFOV without additional support is inefficient in adult patients, there is a lack of studies describing the effects of spontaneous breathing during HFOV on regional lung functions. A recently published study utilizing the DFS investigates the effect of spontaneous breathing on lung aeration and the distribution of ventilation [24]. The results show that spontaneous breathing with DFS during HFOV preserved end-expiratory lung volume, predominantly in the dorsal dependent lung zones, that the use of DFS during HFOV shifted the center of ventilation to the dependent lung zones when compared with HFOV with muscular paralysis, and that there was no indication that spontaneous breaths during HFOV results in regional hyperinflation. Spontaneous breathing during HFOV also improves gas exchange and oxygenation parameters [22]. All of the mentioned effects of spontaneous breathing facilitated by the DFS may have a significant clinical importance. This concept will give HFOV the chance to prove its potential role as early therapy in patients with acute lung injury or acute respiratory distress syndrome [25].

VIII. CONCLUSION

The only system developed so far that effectively supports spontaneous breathing during HFOV was described in this study. First of all, DFS prevents the negative impact of the spontaneous breathing on the ventilator function. In addition, imposed workload of a patient spontaneously breathing through the ventilator circuit is significantly reduced with the DFS. The bench test simulations and the animal experiment suggest that the presented DFS might help to extend the use of HFOV in clinical practice, especially in adult patients.

APPENDIX

Process model parameters:
$R_1 = 2$ kPa·s/L, $R_2 = 0.02$ kPa·s/L, $R_3 = 4$ kPa·s/L,
$C_1 = 1$ L/kPa, $C_2 = 0.15$ L/kPa.
LQ regulator parameters:
$Q_e = 200$, $Q_q = 1$.
Kalman filter parameters:
$\mathbf{W} = \mathrm{diag}([10^5 \quad 10^5])$, $\mathbf{V} = 10^{-2}$.

REFERENCES

[1] L. N. Tremblay and A. S. Slutsky, "Ventilator-induced lung injury: From the bench to the bedside," *Intensive Care Med.*, vol. 32, no. 1, pp. 24–33, Jan. 2006.

[2] C. Putensen, T. Muders, D. Varelmann, and H. Wrigge, "The impact of spontaneous breathing during mechanical ventilation," *Curr. Opin. Crit. Care*, vol. 12, no. 1, pp. 13–18, Feb. 2006.

[3] R. L. Chatburn, "Computer control of mechanical ventilation," *Respir. Care*, vol. 49, no. 5, pp. 507–517, May 2004.

[4] P. Casaseca-de-la-Higuera, F. Simmross-Wattenberg, M. Martin-Fernandez, and C. Alberola-Lopez, "A multichannel model-based methodology for extubation readiness decision of patients on weaning trials," *IEEE Trans. Biomed. Eng.*, vol. 56, no. 7, pp. 1849–1863, Jul. 2009.

[5] F. C. Jandre, A. V. Pino, I. Lacorte, J. H. S. Neves, and A. Giannella-Neto, "A closed-loop mechanical ventilation controller with explicit objective functions," *IEEE Trans. Biomed. Eng.*, vol. 51, no. 5, pp. 823–831, May 2004.

[6] J. Pachl, K. Roubik, P. Waldauf, M. Fric, and V. Zabrodsky, "Normocapnic high-frequency oscillatory ventilation affects differently extrapulmonary and pulmonary forms of acute respiratory distress syndrome in adults," *Physiol. Res.*, vol. 55, no. 1, pp. 15–24, Feb. 2006.

[7] A. B. Froese, "High-frequency oscillatory ventilation for adult respiratory distress syndrome: Let's get it right this time!," *Crit. Care Med.*, vol. 25, no. 6, pp. 906–908, Jun. 1997.

[8] C. N. Sessler, "Sedation, analgesia, and neuromuscular blockade for high-frequency oscillatory ventilation," *Crit. Care Med.*, vol. 33, no. 3, pp. S209–S216, Mar. 2005.

[9] M. van Heerde, H. R. van Genderingen, T. Leenhoven, K. Roubik, F. B. Plotz, and D. G. Markhorst, "Imposed work of breathing during high-frequency oscillatory ventilation: A bench study," *Crit. Care*, vol. 10, no. 1, p. R23, Feb. 2006.

[10] H. E. Fessler, S. Derdak, N. D. Ferguson, D. N. Hager, R. M. Kacmarek, B. T. Thompson, and R. G. Brower, "A protocol for high-frequency oscillatory ventilation in adults: Results from a roundtable discussion," *Crit. Care Med.*, vol. 35, no. 7, pp. 1649–1654, Jul. 2007.

[11] M. van Heerde, K. Roubik, V. Kopelent, F. B. Plotz, and D. G. Markhorst, "Unloading work of breathing during high-frequency oscillatory ventilation: A bench study," *Crit. Care*, vol. 10, no. 4, p. R103, Jul. 2006.

[12] V. Kopelent, "Artificial lung ventilation and its optimization," Ph.D. dissertation, Dept. Radioelectronics, Faculty Elect. Eng., CTU in Prague, Prague, Czech Republic, 2007.

[13] K. J. Astrom and B. Wittenmark, *Computer-Controlled Systems: Theory and Design*, 3rd ed. Upper Saddle River, NJ: Prentice Hall, 1997.

[14] B. D. O. Anderson and J. B. Moore, *Optimal Control: Linear Quadratic Methods*. Mineola, NY: Dover Publications, 2007.

[15] D. Simon, *Optimal State Estimation: Kalman, H Infinity, and Nonlinear Approaches*. Hoboken, NJ: John Wiley and Sons, 2006.

[16] W. Yi, Q. Zhang, Y. Wang, and H. Qin, "Online noninvasive determination of patients and ventilator respiratory work during proportional assist ventilation," in *Proc. 2008 IEEE Int. Conf. Information and Automation*, Zhangjiajie, China, pp. 1163–1167.

[17] M. Terado, S. Ichiba, O. Nagano, and Y. Ujike, "Evaluation of pressure support ventilation with seven different ventilators using Active Servo Lung 5000," *Acta Med. Okayama*, vol. 62, no. 2, pp. 127–133, Apr. 2008.

[18] G. Jiao and J. W. Newhart, "Bench study on active exhalation valve performance," *Respir. Care*, vol. 53, no. 12, pp. 1697–1702, Dec. 2008.

[19] E. Mireles-Cabodevila and R. L. Chatburn, "Work of breathing in adaptive pressure control continuous mandatory ventilation," *Respir. Care*, vol. 54, no. 11, pp. 1467–1472, Nov. 2009.

[20] R. Matejka and K. Roubik, "Advanced monitoring system for conventional and high frequency ventilation," *Lekar a technika*, vol. 38, no. 2, pp. 164–167, June 2008.

[21] A. W. Thille, A. Lyazidi, J.-C. M. Richard, F. Galia, and L. Brochard, "A bench study of intensive-care-unit ventilators: New versus old and turbine-based versus compressed gas-based ventilators," *Intensive Care Med.*, vol. 35, no. 8, pp. 1368–1376, Aug. 2009.

[22] M. van Heerde, K. Roubik, V. Kopelent, F. B. Plotz, and D. G. Markhorst, "Demand flow facilitates spontaneous breathing during high-frequency oscillatory ventilation in a pig model," *Crit. Care Med.*, vol. 37, no. 3, pp. 1068–1073, Mar. 2009.

[23] D. R. Gerstmann, J. M. Fouke, D. C. Winter, A. F. Taylor, and R. A. deLemos, "Proximal, tracheal, and alveolar pressures during high-frequency oscillatory ventilation in a normal rabbit model," *Pediatr. Res.*, vol. 28, no. 4, pp. 367–373, Oct. 1990.

[24] M. van Heerde, K. Roubik, V. Kopelent, M. C. J. Kneyber, and D. G. Markhorst, "Spontaneous breathing during high-frequency oscillatory ventilation improves regional lung characteristics in experimental lung injury," *Acta Anaesth. Scand.*, vol. 54, no. 10, pp. 1248–1256, Nov. 2010.

[25] P. C. Rimensberger, "Allowing for spontaneous breathing during high-frequency oscillation: The key for final success?," *Crit. Care*, vol. 10, no. 4, p. 155, Jul. 2006.

Karel Roubík was born in Náchod, Czech Republic, on May 11, 1971. He received the M. Eng. (Ing.) degree, in 1994, and the Ph.D. degree, in 2001, in radioelectronics from the Czech Technical University in Prague, Faculty of Electrical Engineering; received the Associate Professor (doc.) degree (2006) in biomedical engineering at Technical University in Kosice, Slovakia.

He is currently with the Czech Technical University in Prague, Faculty of Biomedical Engineering in Kladno. His research activities are mainly aimed at artificial lung ventilation and biomedical instrumentation.

Jakub Ráfl (S'11) received the M. Eng (Ing.) degree in electrical and biomedical engineering from the Czech Technical University in Prague, Czech Republic, in 2008, where he is currently working toward the Ph.D. degree in biomedical engineering.

Since 2008, he has been working at the Department of Biomedical Technology, Faculty of Biomedical Engineering, Czech Technical University in Prague, as a Research Assistant. His research is focused on high-frequency oscillatory ventilation.

Marc van Heerde received the M.D. degree from the University of Groningen, Groningen, The Netherlands, in 1998. He completed his training in Pediatrics and Pediatric Intensive Care at the VU University (Vrije Universiteit) Medical Center, Amsterdam, The Netherlands, in 2003 and 2006, respectively.

He is currently working at the Department of Pediatric Intensive Care Unit at the VU University (Vrije Universiteit) Medical Center. In 2006, he started with a Ph.D. project on spontaneous breathing during high-frequency oscillatory ventilation.

Dr. van Heerde was awarded with the John Haven Emerson Award at the conference on high-frequency ventilation, Snowbird, UT, USA, in 2006.

Dick G. Markhorst received the M.D. degree from the VU University (Vrije Universiteit), Amsterdam, The Netherlands, in 1985. He completed his training in pediatrics, neonatology, and pediatric intensive care at the VU University Medical Center, Amsterdam, The Netherlands, in 1992, 1995, and 1997, respectively. In 2005, he received the Ph.D. degree in medicine from the VU University Medical Center. Subject of his thesis was "The optimization of high-frequency ventilation."

He is currently the Head of the Department of Pediatric Intensive Care Unit of the VU University Medical Center. His research focus is on high-frequency oscillatory ventilation.